Surface wave generation due to glacier calving*

doi:10.5697/oc.55-1.101
OCEANOLOGIA, 55 (1), 2013.
pp. 101–127.

KEYWORDS
Glacier calving
Surface waves
Pressure impulse
Integral transforms

Stanisław R. Massel*
Anna Przyborska

Institute of Oceanology,
Polish Academy of Sciences,
Powstańców Warszawy 55, Sopot 81–712, Poland;

e-mail: smas@iopan.gda.pl

*corresponding author

Received 09 September 2012, revised 21 October 2012, accepted 26 November 2012.

Abstract

Coastal glaciers reach the ocean in a spectacular process called 'calving'. Immediately after calving, the impulsive surface waves are generated, sometimes of large height. These waves are particularly dangerous for vessels sailing close to the glacier fronts. The paper presents a theoretical model of surface wave generation due to glacier calving. To explain the wave generation process, four case studies of ice blocks falling into water are discussed: a cylindrical ice block of small thickness impacting on water, an ice column sliding into water without impact, a large ice block falling on to water with a pressure impulse, and an ice column becoming detached from the glacier wall and falling on to the sea surface. These case studies encompass simplified, selected modes of the glacier calving, which can be treated in a theoretical way. Example calculations illustrate the predicted time series of surface elevations for each mode of glacier calving.

* The authors are grateful for support from the Arctic and Environment of the Nordic Seas and the Svalbard-Greenland Area (AWAKE) Grant.

1. Introduction

Loss of land-based ice to the ocean can occur through the melting of glaciers and ice sheets due to direct temperature forcing. Ice can also enter the ocean through changes in the patterns and rates of glacier and ice sheet motion that deliver the ice straight into the ocean. The coastal glaciers in Greenland, Chile, Alaska, Svalbard and the Antarctic reach the ocean in a process called 'calving'. The calving of glaciers is of considerable interest as it is one of the indications of climate warming. Climate warming affects tidewater glaciers through changes in the surface mass balance components and the influence of warmer water on the ice cliff-ocean water interface (Błaszczyk et al. 2009). The greater the transfer of glacier ice from land to the sea, the greater the eustatic sea level rise.

The water into which glaciers calve may be either saline or fresh, or mixed by river and tidal currents. Glaciers are also eroded from below by ocean currents. The growing cavity beneath the ice shelf allows more warm water to melt the ice and subsequently to influence the rise of the global sea level (Stanley et al. 2011).

Most of the papers on calving glaciers have focused on establishing the relation between calving speed and other geometrical and external factors of glaciers. Błaszczyk et al. (2009), for example, discuss the current status of tidewater glaciers in Svalbard, especially in terms of the nature of their calving fronts and dynamic state. According to these authors, the total mass loss due to calving from Svalbard glaciers attains values of 5.0–8.4 $\mathrm{km}^3\ \mathrm{year}^{-1}$, and the average velocity of calving fronts through the archipelago is 20–40 $\mathrm{m\ year}^{-1}$.

Hansson & Hooke (2000) reported that the rate of calving of ground glaciers terminating in water is directly proportional to the water depth. They argued that this process is associated with the oversteepening of the calving face due to differential flow within the ice. Such oversteepening destabilizes the glacier face and facilitates calving.

Because of the inherent danger in obtaining field data to test and construct calving models, Hughes (1992) developed a theory of ice calving for ice walls grounded in water. Slab calving rates from ice walls are controlled by bending creep behind the ice wall, and depend on wall height, forward bending angle and water depth in front of the ice wall. Reasonable agreement was obtained with the calving rates given by Brown et al. (1982) for the Alaskan tide-water glaciers.

Oerlemans et al. (2011) applied the minimal glacier model to study the overall dynamics of the Hansbreen glacier, Svalbard. The ice mechanics were parameterized and a simple law for iceberg calving was used. The

model was calibrated by reconstructing the climate history in such a way that the observed and simulated glacier length match one another.

Using simple energy analysis, MacAyeal et al. (2011) worked out the tsunami source mechanism associated with iceberg capsizing. Such iceberg tsunami generation has been observed at the termini of the Het glacier on Greenland (Amundson et al. 2008, 2010). Immediately after calving, many icebergs capsize owing to the instability of their initial geometry. This process produces impulsive surface waves of large height. Tsunamis generated by sudden iceberg motion have caused severe but localized damage in some Greenland fjords, with harbours destroyed by waves (Levermann 2011). According to MacAyeal et al. (2011), the tsunami crest can reach up to 1% of the initial iceberg height. That is equivalent to about 4 m for an average iceberg from Antarctica (Levermann 2011).

Calving glaciers pose a particular danger to vessels sailing close to the glacier fronts. The Association of Arctic Expedition Cruise Operators has produced Guidelines for Environmental Preservation and Safety in Svalbard. These suggest keeping a distance from the glacier front longer than three times the height of the glacier front. At some glaciers even this distance is too close, so good judgement is needed. The Guidelines note that all glaciers may calve, even if the probability of their doing so differs. Factors that could affect the probability of a calving include the glacier front height, the gradient of the glacier, the speed of the glacier front and the degree of fracturing in the glacier front.

This paper discusses the surface waves generated in front of a glacier as a result of falling ice blocks. To our knowledge, no papers on the theoretical treatment of surface waves caused by glacier calving have been published. As the process of glacier calving is very complicated and cannot be standardized in one type, four case studies of ice blocks falling into water are examined. These case studies encompass simplified, selected modes of glacier calving that can be treated in a theoretical way.

In the first case study, an ice block in the form of a cylinder of radius a and small height b, falls freely without friction on to a calm water surface from a glacier wall of height h_0. This is a case of wave generation due to a pressure impulse on a water surface (see Figure 1). The problem is an extension of the case of a plate or cylinder impacting on a water surface, studied in the past by e.g. Lavrentiev & Shabat (1958), Massel (1967), Cointe & Armand (1987) and Peng & Peregrine (2000).

The second case study deals with a cylindrical column of ice of radius a and height h_0 equal to the height of the glacier wall, sliding freely into calm water with zero initial velocity. This is a case of wave generation following

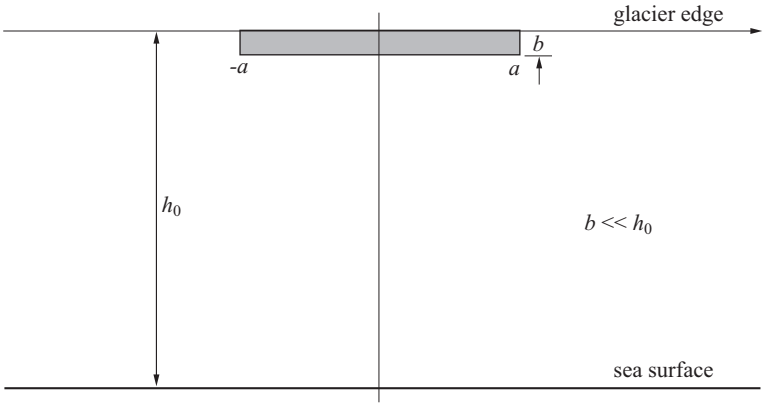

Figure 1. Cylindrical ice block of small thickness impacting on a water surface

the entry of an ice block into the water without a pressure impulse applied at the water surface (see Figure 2).

In the third case, the thickness of the ice block falling on to the sea surface is substantial, although the thickness b satisfies the condition $b < h_0$. Here we have a combination of two wave generation mechanisms, i.e. a pressure impulse on the sea surface and subsequent body entry into the water (see Figure 3). The problem resembles that of waves generated by landslides along coastlines or in enclosed bodies of water, and by the entry

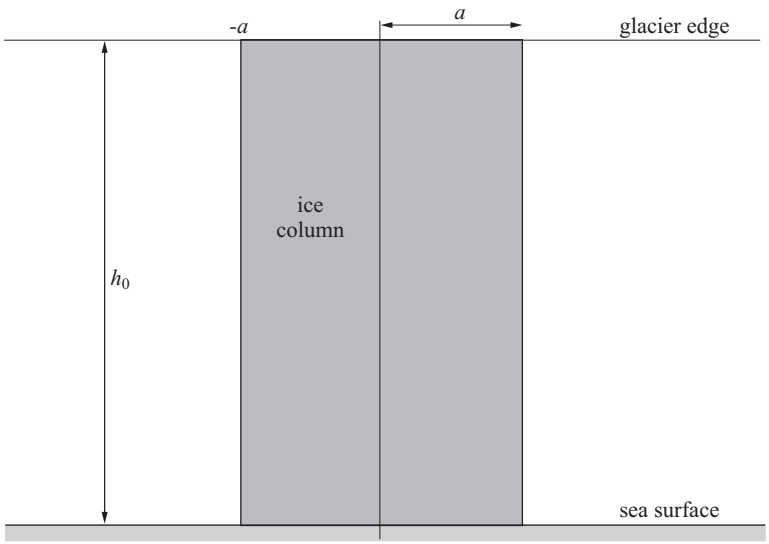

Figure 2. An ice column sliding into water without impact

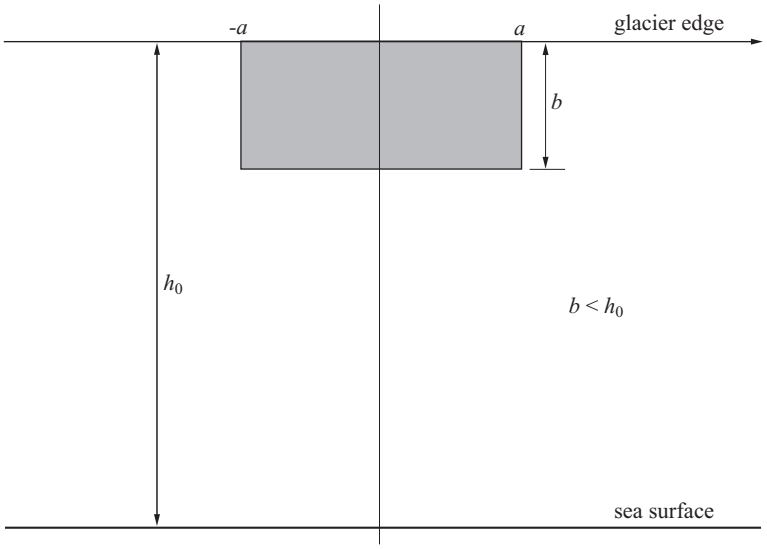

Figure 3. A large circular cylinder impacting on a water surface

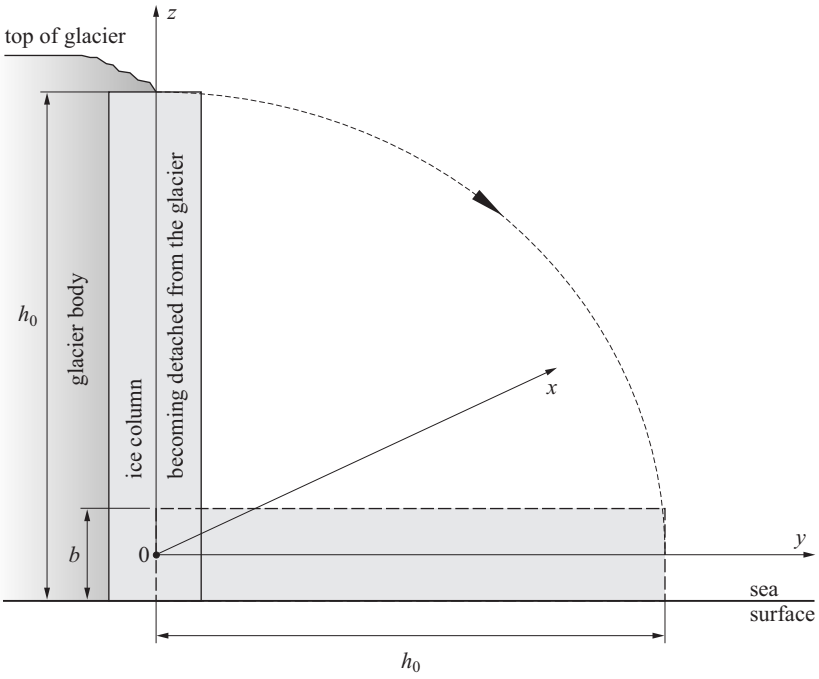

Figure 4. Cross-section of an ice column becoming detached from the glacier wall and impacting on a water surface

of bodies into water (Noda 1970, Di Risio & Sammarco 2008, De Baker et al. 2009).

The last case examines a cylindrical ice column that becomes detached from the glacier wall, rotates around its base on the sea surface, and falls horizontally on to the sea surface with an impact (see Figure 4). The height of the column is equal to the height of the glacier wall.

2. Material and methods

2.1. Governing equations

In order to make the results of the four case studies comparable, it is assumed that the falling ice blocks are cylindrical in shape. It is therefore convenient to introduce the polar coordinate system $O(r,\theta,z)$ with the origin located on the glacier wall at the sea surface (see Figure 5). The sea bed in front of the glacier is horizontal and the water depth is equal to d. During the glacier calving the water is at rest.

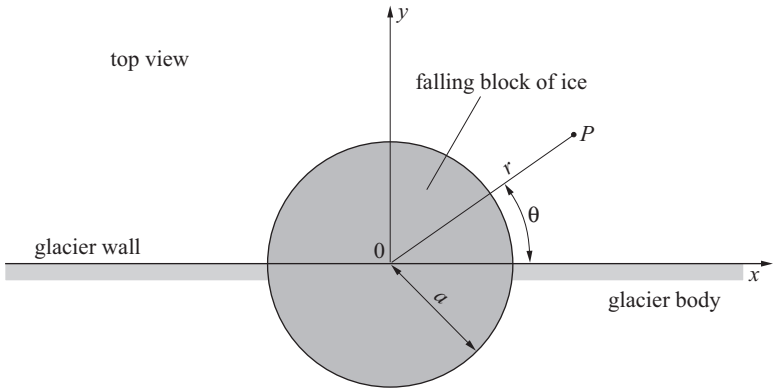

Figure 5. Polar coordinate system

The waves induced by the falling ice block radiate in all directions in the water space ($y > 0$), but the wave-induced velocities, perpendicular to the glacier wall, are equal to zero. We express the water motion due to the impact of the ice block in terms of the velocity potential $\phi(r,z,t)$, satisfying the following linear boundary value problem:

$$\left.\begin{aligned} &\frac{\partial^2\phi}{\partial r^2}+\frac{1}{r}\frac{\partial\phi}{\partial r}+\frac{\partial^2\phi}{\partial z^2}=0\\ &\frac{\partial\phi}{\partial z}=0 \quad \text{at} \quad z=-d\\ &\frac{\partial^2\phi}{\partial t^2}+g\frac{\partial\phi}{\partial z}=0 \quad z=0 \end{aligned}\right\}. \tag{1}$$

The above boundary value problem should make allowance for the relevant initial conditions. However, these conditions depend on the case study under consideration. Therefore in the following Sections, the aforementioned cases will be discussed separately, as the physical mechanisms involved in wave generation are different.

2.2. Cylindrical ice block of small thickness impacting on water

We assume that a rigid cylindrical ice block of radius a and small thickness b falls on to the sea surface (Figure 1). The height of the glacier wall is h_0. When the ice block is falling freely on to the water surface, its velocity v_i close to the sea surface, just before impact, is approximately

$$v_i = \sqrt{2g\left(h_0 - \frac{b}{2}\right)}. \tag{2}$$

On striking the water surface, the ice block creates abrupt forces, which decay shortly afterwards. However, the high loading on the impact region generates a pressure field throughout the water body (Cooker 1996, Peng & Peregrine 2000), and the pressure impulse $p_i(r)$ on the water surface takes the form (Lavrentiev & Shabat 1958)

$$p_i(r) = \begin{cases} \rho_w v_a \sqrt{a^2 - r^2} & r \le a \quad \left[\dfrac{\mathrm{N\,s}}{\mathrm{m}^2}\right] \\ 0 & r > a\ , \end{cases} \tag{3}$$

where v_a is the block velocity after impact and ρ_w is the water density.

After integration of eq. (3) we obtain the force impulse F_i:

$$F_i = \int\limits_S p_i(r)dS = \rho_w v_a \int\limits_0^{2\pi}\int\limits_0^a \sqrt{a^2 - r^2} r\, dr\, d\theta = \frac{2\pi}{3}\,\rho_w\, v_a\, a^3 \quad [\mathrm{N\,s}]. \tag{4}$$

In fact, this force is equal to the change of momentum, before and after impact. Thus we have

$$m(v_i - v_a) = \frac{2\pi}{3}\,\rho_w v_a a^3, \tag{5}$$

in which m is the mass of the ice block

$$m = \pi\rho_i\, a^2 b, \tag{6}$$

where ρ_i is the ice density.

It follows from eq. (5) that the velocity v_a of the ice block after impact becomes

$$v_a = \frac{m v_i}{m + \dfrac{2\pi}{3}\,\rho_w\, a^3} \tag{7}$$

or

$$v_a = \frac{\sqrt{2g\left(h_0 - \dfrac{b}{2}\right)}}{1 + \dfrac{2}{3}\left(\dfrac{\rho_w}{\rho_i}\right)\left(\dfrac{a}{b}\right)}. \tag{8}$$

The above expression indicates that the block velocity after impact is always less than the velocity before impact (Lavrentiev & Shabat 1958, Cooker 1996).

As the thickness of the ice block b is considered to be small, surface wave generation is due mostly to the pressure impulse and not to the body's entry into the water.

When the pressure impulse is prescribed at the free surface, the linear boundary conditions at $z = 0$ become

$$\left.\begin{aligned} \frac{\partial \phi}{\partial z} &= \frac{\partial \zeta}{\partial t} \\ \frac{\partial \phi}{\partial t} + g\zeta &= -\frac{1}{\rho_w}\, p \end{aligned}\right\}. \tag{9}$$

Integration of the pressure impulse over the small time interval $0 \le t \le \tau$ gives (Stoker 1957)

$$\int_0^\tau p\,dt = -\rho_w \phi(r, 0, \tau) - \rho_w\, g \int_0^\tau \zeta\, dt. \tag{10}$$

We assume that when $\tau \to 0$, $p \to \infty$ in such a way that the integral on the left-hand side tends to a finite value – the pressure impulse $p_i(r)$. Since it is natural to assume that ζ is finite, it follows that the integral on the right-hand side vanishes as $\tau \to 0$, and finally we obtain the relationship between the pressure impulse and the initial velocity potential in the form

$$p_i(r) = -\rho_w \phi(r, 0, 0). \tag{11}$$

For later convenience, it is useful to present the general solution of the problem in the form of the Bessel-Fourier integral (Lamb 1932, Massel 2012):

$$\phi(r,z,t) = \Re \int_0^\infty \left(\frac{-ig}{\omega}\right) J_0(kr)\, \frac{\cosh k(z+d)}{\cosh kd}\, A(k) e^{-i\omega t} k\, dk, \tag{12}$$

in which $J_0(x)$ is a Bessel function of the first kind and zero order, $\Re$ denotes the real part of the expression under the integral, and the wave number k satisfies the classical dispersion relation

$$\omega^2 = gk \tanh(kd). \tag{13}$$

The function $A(k)$ is still unknown and should be expressed in terms of the initial boundary conditions.

Like the velocity potential (12), we represent the pressure impulse in the following form:

$$p_i(r) = \int_0^\infty J_0(kr) \int_0^\infty p_i(r_1)\, J_0(kr_1) r_1 dr_1 k dk. \tag{14}$$

After substituting (3) and (12) into (11) for $z = 0$ and $t = 0$, we obtain the unknown function $A(k)$ as

$$\begin{aligned} A(k) &= \frac{-i\omega}{\rho_w g} \int_0^\infty p_i(r_1)\, J_0(kr_1)\, r_1\, dr_1 = \\ &= \frac{-i\omega v_a}{g} \int_0^a \sqrt{a^2 - r_1^2} J_0(kr_1)\, r_1\, dr_1 \end{aligned} \tag{15}$$

or

$$A(k) = \frac{-i\omega\, v_a\, a^3}{g}\, B(ka), \tag{16}$$

where

$$B(ka) = \int_0^1 \sqrt{1-x^2} J_0(kax)\, x dx. \tag{17}$$

Therefore, the velocity potential becomes

$$\phi(r,z,t) = -\alpha a^3\, v_a \int_0^\infty \frac{\cosh k(z+d)}{\cosh kd}\, J_0(kr)\, B(ka)\, \cos\omega t\, k dk. \tag{18}$$

The empirical factor α with a value of the order of 1–2 has been introduced because not all the energy of the falling block is consumed in wave generation in the water space $y > 0$. Moreover, it is difficult to estimate the energy of a falling block that directly induces surface waves subsequently radiating from the impact centre. The remaining part of the energy is consumed in overcoming the friction during the block's fall and in generating forces on the glacier wall. It is clear that in the unlimited space for a freely falling block, the factor $\alpha = 1$. If we take into account the presence of the glacier wall and neglect the energy loss due to friction during the block's fall, $\alpha = 2$, and the total energy is used to generate waves in the half space $y > 0$. The value $\alpha \approx 1.5$, used in this paper, seems to be a reasonable compromise for real situations.

The resulting surface elevation at a given time t and at a radial distance r from the impact origin now becomes

$$\zeta(r,t) = -\alpha \frac{v_a\, a^3}{g} \int_0^\infty J_0(kr)\, B(ka)\, \omega\, \sin(\omega t)\, k dk. \tag{19}$$

The elevations of the surface waves induced by the ice block's impact attenuate with distance from the impact centre, owing to the scattering of wave energy in space; this is expressed by the Bessel function $J_0(kr)$.

The number of parameters influencing the observed surface elevation is very large. For practical applications, therefore, it will be useful to non-dimensionalize the parameters of the glacier and sea basin as follows:

$$\frac{\zeta}{d} = -2\left(\frac{a}{d}\right)^3 \frac{\sqrt{2\left(\frac{h_0}{d}\right) - \left(\frac{a}{d}\right)\left(\frac{b}{a}\right)}}{1 + \frac{2}{3}\left(\frac{\rho_w}{\rho_i}\right)\left(\frac{a}{b}\right)} I_\zeta\left(\frac{r}{d}, \frac{gt^2}{d}, \frac{a}{d}\right) \tag{20}$$

in which

$$I_\zeta\left(\frac{r}{d}, \frac{gt^2}{d}, \frac{a}{d}\right) = \int_0^\infty J_0\left[\left(\frac{r}{d}\right)x\right]\, B\left[\left(\frac{a}{d}\right), x\right] \times$$
$$\times\, \sqrt{x\tanh(x)}\, \sin\left[\sqrt{\left(\frac{gt^2}{d}\right) x\tanh(x)}\right] x dx \tag{21}$$

and

$$B\left[\left(\frac{a}{d}\right), x\right] = \int_0^1 \sqrt{1-y^2}\, J_0\left(\frac{ax}{d}\, y\right) y dy. \tag{22}$$

Recording the surface waves induced by glacier calving is technically very complicated. The fixing of wave staffs at the front of the glacier is almost impossible due to the large water depth and floating ice pieces. Submerged pressure sensors are therfore used in experiments. For relatively long waves they provide a reasonable estimate of the surface elevation. Hence, from equation (18) we obtain the non-dimensional pressure in the form

$$\frac{p}{\rho_w g d} = -2\left(\frac{a}{d}\right)^3 \frac{\sqrt{2\left(\frac{h_0}{d}\right) - \left(\frac{a}{d}\right)\left(\frac{b}{a}\right)}}{1 + \frac{2}{3}\left(\frac{\rho_w}{\rho_i}\right)\left(\frac{a}{b}\right)} I_p\left(\frac{r}{d}, \frac{gt^2}{d}, \frac{a}{d}, \frac{z}{d}\right) \tag{23}$$

in which

$$I_p\left(\frac{r}{d}, \frac{gt^2}{d}, \frac{a}{d}, \frac{z}{d}\right) = \int_0^\infty J_0\left[\left(\frac{r}{d}\right)x\right] B\left[\left(\frac{a}{d}\right)x\right] \frac{\cosh\left[\left(1+\frac{z}{d}\right)x\right]}{\cosh(x)} \times$$
$$\times \sqrt{x\tanh(x)} \sin\left[\sqrt{\left(\frac{gt^2}{d}\right)x\tanh(x)}\right] x dx. \tag{24}$$

2.3. An ice column sliding into the water without impact

2.3.1. Dynamics of the ice block

Now we assume that a cylindrical ice column of height h_0 (see Figure 2) starts to slide vertically into the water from its initial position when the bottom of the ice block is initially in line with the water surface. The motion of the block is non-stationary. At first, the block accelerates, but after some time the block's velocity decreases and changes direction, oscillating vertically with attenuating amplitude. When the resulting force vanishes and the block's velocity drops to zero, the ice block reaches its neutral submergence.

In the early stages of motion, the vorticity does not have enough time to diffuse. Hence, the boundary layers are very thin, the flow is essentially irrotational (Sarpkaya & Isaacson 1981), and the fluid forces acting on the body consist of drag and inertia forces. The overall drag of a body is usually separated into two components – pressure drag and friction drag. Pressure drag is a consequence of the separation of the streamlines. However, this is not the case for an ice block sliding into water when the upper part of the block usually appears above water. It is therefore reasonable to assume

that almost all the drag is due to shear stress in the boundary layer over the ice block surface. The drag due to friction therefore becomes

$$F_{\mathrm{d,friction}} = \frac{1}{2}\, C_{\mathrm{d,friction}}\, S_{\mathrm{circ}}(t) v(t) \mid v(t) \mid, \tag{25}$$

where $C_{\mathrm{d,friction}}$ is the frictional drag coefficient, and the wetted area of the cylinder submerging into the water is $S_{\mathrm{circ}} = 2\pi a\ s(t)$, where $s(t)$ is the submergence of the ice block bottom at a given time t, i.e.

$$s(t) = \int_0^t v(t)\, dt. \tag{26}$$

The value of $C_{\mathrm{d,friction}}$ is not known: it depends on the boundary layer flow regime and on the roughness of the ice block surface. In order to estimate the value of $C_{\mathrm{d,friction}}$ let us consider the resemblance of the very great roughness of the ice block surface with the rough surface of some vegetated sea bottom, for example, the surface of a coral reef. Nelson (1996) showed that for such a surface, the frictional drag coefficient $C_{\mathrm{d,friction}}$ is of the order of 0.1–0.2. However, as the ice block surface is probably much rougher we have adopted the value $C_{\mathrm{d,friction}} = 0.50$ in the calculations.

The second part of the force induced by the fluid on the accelerating ice block, namely the inertia force, is

$$F_{\mathrm{inertia}} = \rho_w C_a V_s(t) \frac{dv(t)}{dt}, \tag{27}$$

in which $V_s(t) = \pi a^2 s(t)$ is the volume of the submerged part of ice block and C_a is the inertia coefficient. Newman (1977) argued that the added mass for elongated bodies moving in a fluid is very small in comparison with the body mass. In particular, when the ratio $\epsilon = R/l << 1$, where R is the body radius and l is the body length, the added mass coefficient $C_a \approx \epsilon^2 \ln \epsilon$. Thus if the radius of the ice block $R \approx 5$ m and its length ≈ 40 m, we obtain $C_a \approx 0.25$.

In general, when an ice block is submerging into water, the mass of the 'wet' block increases and the ratio of the length $s(t)$ to the block radius a changes in time. Hence, the coefficient C_a will also change for each position of the block in the water. To obtain some insight into the time evolution of the coefficient C_a during the block's submerging, we will assume for a moment that the submerged part of the ice block has the shape of an ellipsoid of revolution

$$\frac{x^2}{a^2} + \frac{y^2}{a^2} + \frac{z^2}{\left(\frac{s(t)}{2}\right)^2} = 1, \tag{28}$$

where x and y are the horizontal axes, and z is the vertical axis. Lamb (1932) showed theoretically that for different values of the ratio $(0.5\,s(t))/a$ of an ellipsoid of revolution, the coefficient C_a decreases monotonically from $C_a = 0.5$ for $(0.5\,s(t))/a = 1.0$ to $C_a = 0.021$ for $(0.5\,s(t))/a = 10.0$. This attenuation can be given by the approximate formula

$$C_a = 0.5\left(\frac{s(t)}{2a}\right)^{-1.265}. \tag{29}$$

However, in this paper the constant value of $C_a \approx 0.25$, being a reasonable compromise for the case of a falling ice block, will be used. This value results from Newman's estimate and also corresponds to the mean value given by equation (29).

To calculate the velocity time series of the ice block's motion, let us formulate the balance equation of all the forces involved, namely, the ice block weight W, buoyancy force $B(t)$ and resistance force $R(t)$. Thus for the z axis, directed downwards, we have

$$\rho_i\, V_i\, \frac{dv(t)}{dt} = W - B(t) - R(t), \tag{30}$$

in which

$$W = \rho_i\, V_i\, g \qquad \text{and} \qquad B(t) = \rho_w\, V_s(t)\, g, \tag{31}$$

and

$$R(t) = \frac{1}{2}\rho_w C_{\mathrm{d,friction}} S_{\mathrm{circ}} v(t)|v(t)| + \rho_w C_a V_s(t)\frac{dv(t)}{dt}, \tag{32}$$

where V_i is the volume of the ice block, $V_i = \pi a^2 h_0$.

Using eq. (31) and (32), we rewrite eq. (30) in the form

$$\frac{dv}{dt} = A(t) - B(t)v(t)|v(t)|, \tag{33}$$

where

$$A(t) = \frac{g\left[1 - \left(\frac{\rho_w}{\rho_i}\right)\left(\frac{s(t)}{h_0}\right)\right]}{1 + \left(\frac{\rho_w}{\rho_i}\right) C_a \left(\frac{s(t)}{h_0}\right)} \tag{34}$$

and

$$B(t) = \frac{C_{\mathrm{d,friction}}\left(\frac{\rho_w}{\rho_i}\right)\left(\frac{s(t)}{ah_0}\right)}{1 + \left(\frac{\rho_w}{\rho_i}\right) C_a \left(\frac{s(t)}{h_0}\right)}. \tag{35}$$

Eq. (33) should be solved for the following initial boundary conditions

$$s(t) = 0, \quad v(t) = 0 \qquad \text{for} \qquad t = 0. \tag{36}$$

2.3.2. Surface waves due to an ice column sliding into water without impact

A cylindrical ice block submerging into water behaves like a plunger-type wave-maker (Noda 1970) without the generation of a pressure impulse (the initial velocity of the ice block is equal to zero). To study the surface waves generated due the ice block's motion, we assume that the origin of the cylindrical coordinate system $O(r, \theta, z)$ is located at the water surface and that the z axis is directed downwards. At the initial time $t = 0$, the bottom of the ice block is located at level $z = 0$ and its velocity $v(t) = 0$. As the ice block moves into the water, the boundary condition at its surface becomes

$$u(z,t) = \frac{\partial \phi}{\partial r} = 0 \quad \text{at} \quad t > 0 \quad \text{and} \quad z < s(t), \tag{37}$$

where $u(z,t)$ is the outward velocity, normal to the ice block surface.

The velocity $u(z,t)$ under the ice block, when $(s(t) < z < d)$, can be determined approximately from the principle of conservation of mass, when some vertical profile of the velocity $u(z,t)$ radiating outwards is assumed. Therefore on the total immersed 'virtual' cylindrical surface $(r = a)$ we have

$$u(z,t) = \frac{\partial \phi}{\partial r} = \begin{cases} 0, & z \le s(t) \\ F(z, s(t)), & s(t) < z \le d. \end{cases} \tag{38}$$

Function $F(z, s(t))$ is still unknown. It will be determined later, depending on the prescribed vertical profile of velocity $u(z,t)$ under the ice block.

Wave generation due to submergence of the ice block is an irrotational, non-stationary process, starting from rest at time $t = 0$. Therefore, in order to find the corresponding velocity potential of the generated waves for $t > 0$, we apply the Laplace Transform for the potential $\phi(r, z, t)$, as follows (Abramowitz & Stegun 1975)

$$\overline{\phi}(r, z, p) = \int_0^\infty \phi(r, z, t)\, e^{-pt}\, dt, \quad p > 0. \tag{39}$$

The boundary value problem after the Laplace Transform becomes (Ghosh 1991)

$$\frac{\partial^2 \overline{\phi}}{\partial r} + \frac{1}{r}\frac{\partial \overline{\phi}}{\partial r} + \frac{\partial^2 \overline{\phi}}{\partial z^2} = 0, \quad a < r < \infty, \quad 0 < z < d, \tag{40}$$

$$\frac{\partial \overline{\phi}}{\partial z} = 0, \quad z = d \tag{41}$$

$$p^2\overline{\phi} - g\,\frac{\partial\overline{\phi}}{\partial z} = 0, \quad z = 0, \tag{42}$$

$$\frac{\partial\overline{\phi}}{\partial r} = \overline{u}(z,p), \quad r = a, \tag{43}$$

$$\frac{\partial\overline{\phi}}{\partial z} = 0, \quad z = d, \tag{44}$$

where $\overline{u}(z,p)$ is the Laplace Transform of the normal velocity $u(z,t)$.

However, the boundary value problem should be solved in the finite domain (a,∞) and boundary condition (43) should be applied at the cylindrical ice block surface, with the velocity changing along the z axis. Therefore, we make another transformation using the Weber Transform (Piessens 1996) for the horizontal distance r, i.e.

$$\overline{\varphi}(\xi,z,p) = \int_a^\infty r\,a\;(r,\xi)\,\overline{\phi}(r,z,p)\,dr, \tag{45}$$

in which

$$A(r,\xi) = J_1(a\xi)\,Y_0(r,\xi) - J_0(r\xi)\,Y_1(a\xi), \tag{46}$$

where J_n and Y_n are Bessel functions of the first and second kinds respectively.

Giving the Bessel functions in terms of Hankel functions and taking the Laplace and Weber Transform inversions, we obtain the velocity potential $\phi(r,z,t)$ in the form (Ghosh 1991)

$$\phi(r,z,t) = -\Re\left(\frac{1}{\pi i}\int_0^\infty B(r,k)\,[E_1(k) + E_2(k)]\right)dk \tag{47}$$

in which

$$E_1(k) = \frac{\sinh(kz)}{\cosh(kd)}\int_0^d \frac{\cosh[k(d-y)]u(y,t)}{k}dy, \tag{48}$$

$$E_2(k) = \frac{2\omega\cosh[k(d-z)]}{k\sinh(2kd))}\int_0^d \cosh[k(d-y)]\int_0^t u(y,\tau)\,\sin[\omega(t-\tau)]d\tau dy, \tag{49}$$

$$B(ka,kr) = \frac{H_0^{(1)}(kr)}{H_1^{(1)}(ka)} - \frac{H_0^{(2)}(kr)}{H_1^{(2)}(ka)} \tag{50}$$

and

$$\omega = \sqrt{gk\,\tanh(kd)}. \tag{51}$$

The Hankel functions are defined as follows (Abramowitz & Stegun 1975):

$$H_n^{(1)}(z) = J_n(z) + iY_n(z) \quad \text{for} \quad n = 0, 1 \tag{52}$$

$$H_n^{(2)}(z) = J_n(z) - iY_n(z) \quad \text{for} \quad n = 0, 1. \tag{53}$$

Let us now determine the unknown function $F(y, s(t))$ describing the radiating velocity $u(y,t)$ on the 'immersed' vertical cylinder at $r = a$. Two proposed profiles are prescribed as follows:

Profile 1: velocity $u(y,t)$ is uniformly distributed along y axis for $s(t) < y < d$

Hence the principle of conservation of mass gives

$$\pi a^2\, v(t) = 2\pi a\, [d - s(t)]\, u(t) \tag{54}$$

or

$$u(t) = \frac{a}{2[d - s(t)]}\, v(t), \tag{55}$$

where $v(t)$ is given by the solution of eq. refeq28).

Profile 2: velocity $u(y,t)$ attenuates linearly with coordinate y for $s(t) < y < d$

This hypothetical attenuation of the radiating horizontal velocity $u(y,t)$ can appear as a result of possible turbulence of the water under the falling ice block and the aeration of the water mass. The balance of the mass of water yields the radiating velocity in the form

$$u(y,t) = \frac{a(d-y)}{[d - s(t)]^2}\, v(t). \tag{56}$$

Using the velocity potential (47) we obtain the time series of the surface elevation in the form

$$\zeta(r,t) = -\frac{1}{g}\frac{\partial \phi(r,0,t)}{\partial t} \tag{57}$$

or

$$\zeta(r,t) \;\; = \;\; \Re\, \frac{1}{\pi i} \int_0^\infty \frac{B(r,k)}{\cosh(kd)} \times$$

$$\times \int_0^t \cos[\omega(t-\tau)] \left(\int_0^d u(y,\tau) \cosh[k(d-y))] dy \right) d\tau dk. \tag{58}$$

This general expression for the surface elevation depends on the velocity profile of the radiating velocity $u(y,t)$. Hence, we obtain the following expressions for the surface elevations for particular radiating velocity profiles:

$$\begin{aligned} \zeta_1(r,t) &= \Re \frac{1}{\pi i} \int_0^\infty \frac{B(r,k)}{\cosh(kd)} \times \\ &\times \int_0^t C_1(\tau)\, v(\tau) \cos[\omega(t-\tau)] d\tau dk, \end{aligned} \tag{59}$$

where

$$C_1(\tau) = a\, \frac{\sinh[k(d-s(\tau))]}{2k(d-s(\tau))} \tag{60}$$

and

$$\begin{aligned} \zeta_2(r,t) &= \Re \frac{1}{\pi i} \int_0^\infty \frac{B(r,k)}{\cosh(kd)} \times \\ &\times \int_0^t C_2(\tau)\, v(\tau) \cos[\omega(t-\tau)] d\tau dk, \end{aligned} \tag{61}$$

where

$$C_2(\tau) = a\, \frac{k[d-s(\tau)] \sinh[k(d-s(\tau))] - \cosh[k(d-s(\tau))] + 1}{[k(d-s(\tau))]^2}. \tag{62}$$

It should be noted that the similar one-dimensional problem of the surface wave generation in a the laboratory flume was solved by De Risio & Sammarco (2008) by applying the Laplace and Fourier Transforms.

2.4. A large ice block falling on to water with a pressure impulse

Such a case is illustrated schematically in Figure 3. In contrast to Figure 1, the thickness b of the block is a substantial part of the glacier wall. This means that the surface waves will be generated by two mechanisms. Firstly, on touching the water surface, the block induces a pressure impulse

and subsequently generates surface waves. Next, submergence of the ice block into the water and its vertical oscillations provides the second generation mechanism. Thus we can write

$$\zeta(r,t) = \zeta_{\text{imp}}(r,t) + \zeta_{\text{sub}}(r,t), \tag{63}$$

where $\zeta_{\text{imp}}(r,t)$ is the surface oscillation due to the pressure impulse and $\zeta_{\text{sub}}(r,t)$ is the surface oscillation due to block's submergence.

The surface elevation $\zeta_{\text{imp}}(r,t)$ is given by eq. (19). After impact on the sea surface, the ice block oscillates vertically in the water, radiating surface waves in the space $y > 0$. The governing equation for the velocity of the oscillating ice block is similar to eq. (33), where $A(t)$ and $B(t)$ become

$$A(t) = \frac{g\left[1 - \left(\frac{\rho_w}{\rho_i}\right)\left(\frac{s(t)}{b}\right)\right]}{1 + \left(\frac{\rho_w}{\rho_i}\right) C_a \left(\frac{s(t)}{b}\right)} \tag{64}$$

and

$$B(t) = \frac{C_{\text{d,friction}}\left(\frac{\rho_w}{\rho_i}\right)\left(\frac{s(t)}{ab}\right)}{1 + \left(\frac{\rho_w}{\rho_i}\right) C_a \left(\frac{s(t)}{b}\right)}. \tag{65}$$

However, the initial conditions are now

$$s(t) = 0, \quad v(t) = v_a \qquad \text{for} \qquad t = 0. \tag{66}$$

2.5. An ice column becoming detached from the glacier wall and falling on to water

When a calving glacier moves seawards, an ice column sometimes becomes detached from the glacier wall and falls on to the water. To model this process we assume that the vertical ice column has a height h_0 and that the cross-section of the block is $(2a \times b)$, where $2a$ is the width of the ice block along the glacier wall (x axis) and b is the block's thickness. We assume that the detached ice block rotates around its base and impacts horizontally on the sea surface (see Figure 4). Taking into account the previous results, which indicate that for a small column thickness the wave heights due to impact are much bigger than those due to the oscillations of the submerged ice block, only wave generation due to pressure impulse is considered.

Under natural conditions, the motion of a detaching and rotating ice block is very complicated. To parameterize this process we assume that the ice block starts to rotates around its base as one rigid piece of ice with the

same constant angular frequency ω. Thus, at the instant the block touches the sea surface, its velocity, normal to the sea surface, becomes

$$v_i(y) = \omega y, \quad 0 < y < h_0, \tag{67}$$

where y is the distance along the falling ice block (see Figure 4).

As in equation (3), the pressure impulse $p_i(x, y)$ can be written thus:

$$p_i(x, y) = \rho_w \, v_a(y) \sqrt{a^2 - x^2}. \tag{68}$$

To calculate the ice block's velocity $v_{\mathrm{a}}(y)$ after impact we write the change of momentum in the form:

$$\int_0^{h_0} m[v_i(y) - v_a(y)]dy = \int_0^{h_0} \int_{-a}^{a} p_i(x, y)dx \, dy. \tag{69}$$

After substituting eqs. (67) and (68) into equation (69) we obtain

$$v_a(y) = \frac{\omega y}{1 + \frac{\pi}{4}\left(\frac{\rho_w}{\rho_i}\right)\left(\frac{a}{b}\right)}. \tag{70}$$

Using equation (70) and integrating the pressure impulse $p_i(x, y)$, we obtain the force impulse F_i as follows:

$$F_i = \int_0^{h_0} \int_{-a}^{a} \rho_w \frac{\omega y}{1 + \frac{\pi}{4}\left(\frac{a}{b}\right)\left(\frac{\rho_w}{\rho_i}\right)} \sqrt{a^2 - x^2} \, dx \, dy = \frac{\pi}{4} \frac{\rho_w \omega a^2 h_0^2}{1 + \frac{\pi}{4}\left(\frac{a}{b}\right)\left(\frac{\rho_w}{\rho_i}\right)}. \tag{71}$$

The wave surface pattern in the region close to the impacting ice block is very complicated. On the other hand, far from the area of impact, the influence of the shape of the impacting body on the observed wave pattern is not important. Therefore, for the convenience of the later calculations, we define the radius a_e of an equivalent cylindrical ice block in such a way that the area of the impacting ice block and the area of the cylindrical block touching the water surface are the same. Thus, for an equivalent cylindrical block radius a_e we obtain

$$2ah_0 = \pi a_e^2 \tag{72}$$

and

$$a_e = \sqrt{\frac{2ah_0}{\pi}}. \tag{73}$$

Additionally, the corresponding equivalent velocity v_a of the cylindrical block is determined from the condition that the force impulse F_i for both cases is the same. Therefore, by equating force impulses (4) and (71), we obtain the equivalent velocity $v_{a,e}$ in the form

$$v_{a,e} = \frac{3(\pi)^{3/2}}{16\sqrt{2}} \frac{\omega\sqrt{ah_0}}{1 + \dfrac{\pi}{4}\left(\dfrac{\rho_w}{\rho_i}\right)\left(\dfrac{a}{b}\right)}. \tag{74}$$

Hence, the problem of surface waves generated by an ice column becoming detached from a glacier wall has been reduced to the case of the impact of an equivalent cylindrical ice block of radius a_e and of small thickness.

3. Results and discussion

The final results of the hydrodynamic models, obtained above, are given in the form of time series of surface elevations as functions of time and distance. The models suggest the very intense attenuation of the wave amplitude generated by glacier calving for all the modes discussed. In order to quantify this attenuation let us illustrate the derived formulae with some numerical examples. First, we consider the case of a cylindrical ice block of small thickness impacting on water. The following parameters are used in the calculations: the radius a and thickness b of the ice block are equal to 5 m and 2 m respectively; the glacier wall height $h_0 = 50$ m; the water depth in

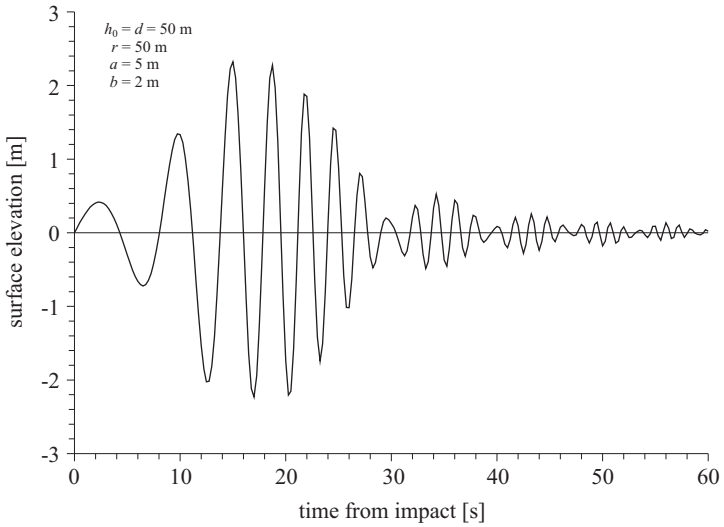

Figure 6. Time series of sea surface elevation at distance $r = 50$ m from the impact centre. An ice block of small thickness

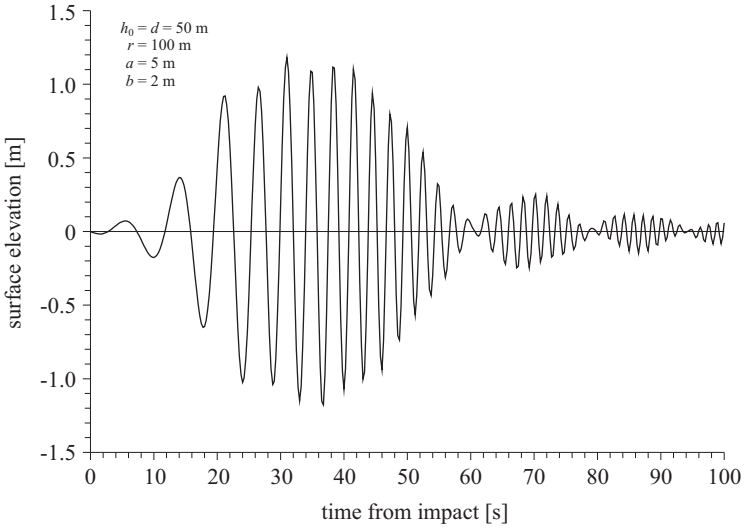

Figure 7. Time series of sea surface elevation at distance $r = 100$ m from the impact centre. An ice block of of small thickness

front of the glacier wall $d = 50$ m; the density of water $\rho_w = 1024$ kg m^{-3}; and the density of ice $\rho_i = 916$ kg m^{-3}. The velocity of the falling block before impact is $v_i = 30.99$ m s^{-1} whereas after impact the velocity $v_a = 9.46$ m s^{-1}. The resulting force impulse is $F_i = 2.53 \times 10^6$ N s. Figure 6 shows the time series of the surface elevation for distance $r = h_0 = 50$ m, is shown. The maximum wave amplitude is ca 2.32 m, attenuating rapidly in time. At distance $r = 2 \times h_0 = 100$ m the maximum amplitude is reduced to about 1.25 m (see Figure 7).

Figures 8 and 9 illustrate the vertical velocity of block oscillation and its submergence for a cylindrical block of height $h_0 = 50$ m and radius $a = 5$ m sliding quietly into water of depth $d = 50$ m (the second mode of glacier-calving). The inertia coefficient $C_a = 0.25$ and the friction drag coefficient $C_{\mathrm{d,friction}} = 0.50$ were used in the calculations. Because of the many holes and cracks in the ice block, an ice density $\rho_i \approx 750$ kg m^{-3} was adopted. This value is smaller than the theoretical one of $\rho_i = 916$ kg m^{-3} for an ice block without holes or cracks. Having slid into the water, the block oscillates vertically with diminishing velocity. The maximum downward velocity is equal to 12.28 m s^{-1} and the maximum upward velocity is 2.50 m s^{-1} (see Figure 8f). After about 100 s the ice block reaches its neutral position (see Figure 9f). From this Figure it follows that the submergence of the block bottom at equilibrium is equal to about $\left(\frac{\rho_i}{\rho_w}\right) h_0 \approx 36.62$ m, whereas the maximum submergence of the block bottom is 44.35 m.

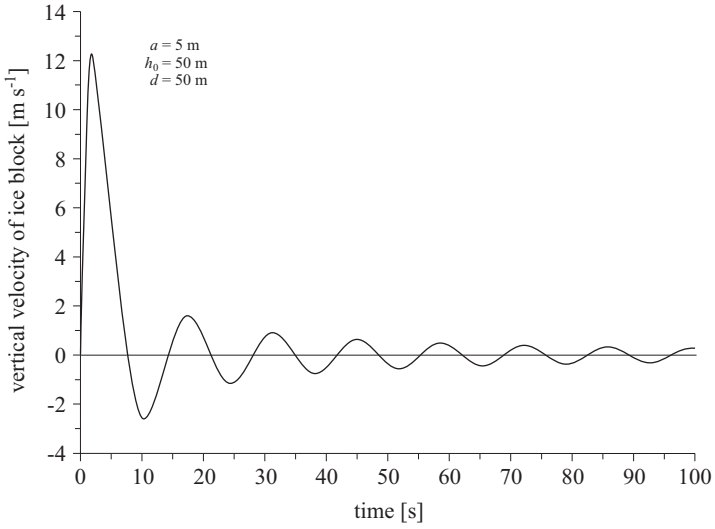

Figure 8. Time series of the vertical velocity of an oscillating ice column after sliding into water

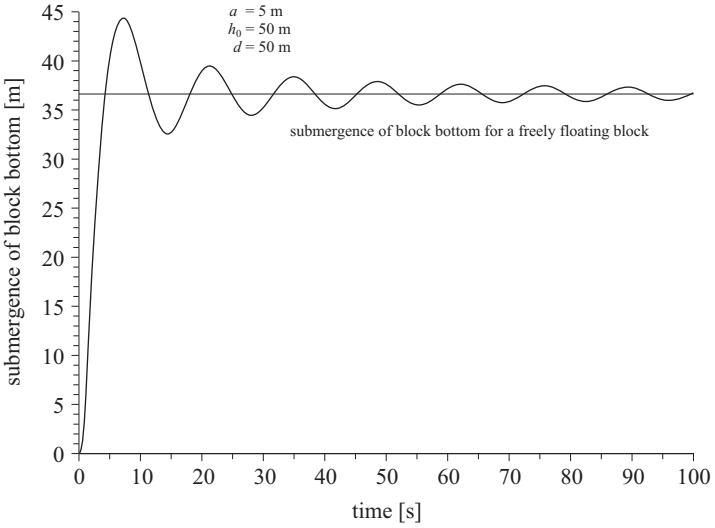

Figure 9. Time series of the submergence of the bottom an ice column after sliding into water

The corresponding time series of the water surface oscillations at $r =$ 25 m from the impact centre is given in Figure 10. The two profiles of the radiating velocity (see eqs. (55) and (56)) result in similar surface elevations. Comparison of the surface elevations due to the ice block impact (see Figure 6) and due to an ice block sliding quietly into the water, without

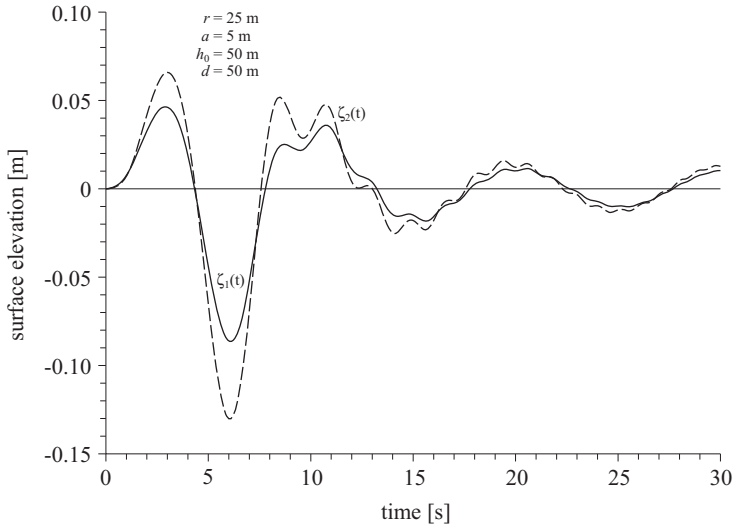

Figure 10. Time series of sea surface elevation at distance $r = 25$ s from the impact centre. Ice column sliding into water

impact (see Figure 10), shows that in the latter case the waves are much smaller. This is because the normal radiating velocity $u_{\text{norm}}(z,t)$ (see eq. (38)), being the forcing factor for the generation of surface oscillations, is very small.

The third glacier calving mode illustrates the case of a large ice block falling on to the sea surface with a pressure impact and subsequently submerging into the water. If we assume that a cylindrical ice block of radius $a = 5$ m and thickness $b = 10$ m falls from the top of a glacier wall of height $h_0 = 50$ m, its velocity before impact becomes $v_i = 29.7$ m s^{-1} and its velocity after impact $v_a = 17.6$ m s^{-1}, while the impulse force generated by the impact is equal to 4.7×10^6 Ns. The time history of surface oscillations $\zeta_{\text{imp}}(t)$ at a radial distance $r = 50$ m from the impact centre is shown in Figure 11. The maximum elevation of the water surface ($\zeta_{\max} \approx 5.1$ m) appears at $t \approx 15$ s from the impact. The surface elevation component due to ice block oscillations is negligibly small and is not shown in the figure.

The last mode of glacier calving involves an ice column becoming detached from the glacier wall and falling freely on to the water surface. Let us therefore consider a slab of ice of cross-section $2a \times b$, where $2a = 10$ m and $b = 5$ m. The length of the ice column $h_0 = 50$ m and the frequency of the falling block rotation $\omega = 1$ Hz. The calculations show that the equivalent radius of the cylindrical ice block $a = 12.61$ m and the equivalent velocity $v_{a,e} = 6.21$ m s^{-1}. Figure 12 illustrates the time series of the surface elevations at distance $r = 50$ m from the impact centre.

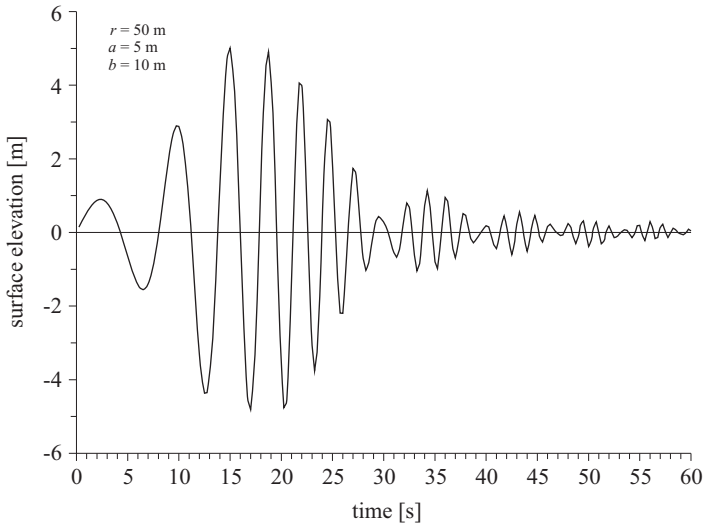

Figure 11. Time series of surface oscillations at distance $r = 50$ m from the impact centre due to a large ice block falling on to the water surface with pressure impulse. The component of surface elevation due to ice block oscillations is negligible small and is not shown in the Figure

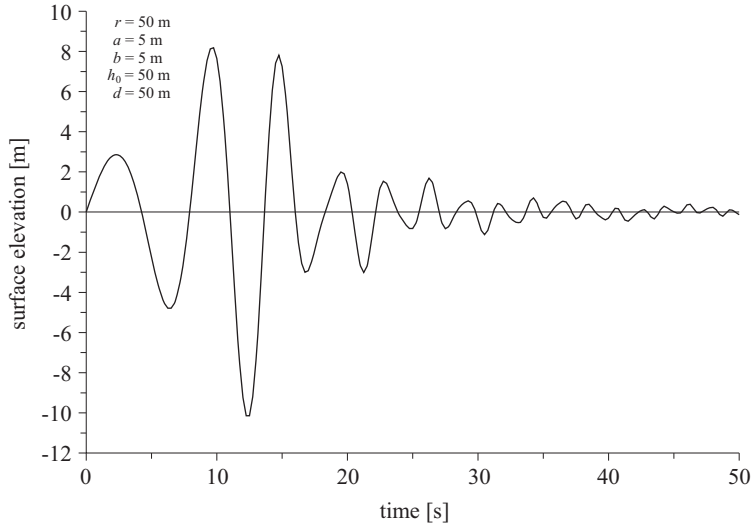

Figure 12. Time series of surface oscillations at distance $r = 50$ m due to an ice column becoming detached from the glacier wall and falling on to the water surface

Table 1 summarizes the maximum amplitudes of surface elevations induced by all the modes of glacier calving discussed in this paper for three

Table 1. Maximum amplitudes for particular modes of glacier calving at selected distances from the glacier wall

Modes of calving	Max. amplitude [m]		
	$r = h_0 = 50$ m	$r = 2h_0 = 100$ m	$r = 3h_0 = 150$ m
impact of a cylindrical ice block of small thickness: $a = 5$ m, $b = 2$ m	2.32	1.25	0.80
ice column sliding into water without a pressure impulse: $a = 5$ m, $h_0 = 50$ m	0.06	0.04	0.03
large ice block falling on to water with a pressure impulse: $a = 5$ m, $b = 10$ m	5.10	2.60	1.70
ice column becoming detached from a glacier wall and falling on to water with a pressure impulse: $2a = 10$ m, $b = 5$ m	8.18	5.60	3.54

distances from the glacier wall: $r = h_0, r = 2h_0$, and $r = 3h_0$. In particular, four cases of glacier calving have been considered: a cylindrical ice block of small thickness impacting on water, an ice column sliding quietly into water without impact, a large ice block falling on to water with a pressure impulse, and an ice column becoming detached from the glacier wall and falling on to the water surface. Comparison of the maximum amplitudes shows that in the case of the ice column becoming detached from the glacier wall and falling on the sea surface, the generated waves are higher than for the other calving modes. On the other hand, an ice column sliding into the water and subsequently oscillating there generates very small surface waves. The mechanism whereby water is thrust out from beneath the ice block appears to be very ineffective in surface wave generation.

The theory developed here may be useful for estimating the wave amplitude as a function of distance from the glacier wall, and as a function of time from the impact at a given location. The interesting reverse problem of estimating the volume of a falling block of ice, when the time series of surface oscillations or dynamic pressure at a given distance from the glacier wall are known, will be treated in a separate paper.

Acknowledgements

We would like to thank the reviewers for their useful comments and suggestions.

References

Abramowitz M., Stegun I. A., 1975, *Handbook of mathematical functions*, Dover Publ., New York, 1045 pp.

Amundson J. M., Truffer M., Lutki M. P., Fahnestock M., West M., Motyka R. J., 2008, *Glacier, fjord, and seismic response to recent large calving events, Jakobshavn Isbrae, Greenland*, Geophys. Res. Lett., 35 (22), http://dx.doi.org/10.1029/2008GL035281.

Amundson J. M., Fahnestock M., Truffer M., Brown J., Lutki M. P., Motyka R. J., 2010, *Ice mélange dynamics and implications for terminus stability, Jakobshavn Isbrae, Greenland*, J. Geophys. Res., 115 (F1), 12 pp., http://dx.doi.org/10.1029/2009JF001405.

Błaszczyk M., Jania J. A., Hagen J. O., 2009, *Tidewater glacier of Svalbard: recent changes and estimates of calving fluxes*, Pol. Polar Res., 30 (2), 85–142.

Brown C. S., Meier M. F., Post A., 1982, *Calving speed of Alaska tidewater glaciers, with application to Columbia Glacier*, U.S. Geol. Surv. Prof. Pap., 1258-C.

Cointe R., Armand J. L., 1987, *Hydrodynamic impact analysis of a cylinder*, J. Offshore Mech. Arctic Eng., 109 (3), 237–243, http://dx.doi.org/10.1115/1.3257015.

Cooker M. J., 1996, *Sudden changes in a potential flow with a free surface due to impact*, Q. J. Mech. Appl. Math., 49, 581–591, http://dx.doi.org/10.1093/qjmam/49.4.581.

De Backer G., Vantorre M., Beels C., De Pre J., De Rouck J., Blommaert C., Van Paepegem W., 2009, *Experimental investigation of water impact of axisymmetric bodies*, Appl. Ocean Res., 31 (3), 143–156, http://dx.doi.org/10.1016/j.apor.2009.07.003.

De Risio H., Sammarco P., 2008, *Analytical modeling of landslide-generated waves*, J. Waterw. Port C. Div., 134 (1), 53–60, http://dx.doi.org/10.1061/(ASCE)0733-950X(2008)134:1(53).

Glosh N. K., 1991, *A cylindrical wave-maker problem in a liquid of finite depth with an inertial surface in the presence of surface tension*, J. Austral. Math. Soc., Ser. B, 111–121.

Hanson B., Hooke R. L., 2000, *Glacier calving: a numerical model of forces in the calving-speed/water-depth relation*, J. Glaciol., 46 (153), 188–196, http://dx.doi.org/10.3189/172756500781832792.

Hughes T., 1992, *Theoretical calving rates from glaciers along ice walls grounded in water of variable depths*, J. Glaciol., 38 (129), 282–294.

Lamb H., 1932, *Hydrodynamics*, Dover Publ., London, 738 pp.

Lavrentiev M. A., Shabat B. V., 1958, *Methods of theory functions of complex variables*, Gos. Izd. Fiz-Math. Moscow, 678 pp., (in Russian).

Levermann A., 2011, *When glacial giants roll over*, Nature, 472 (7341), 43–44, http://dx.doi.org/10.1038/472043a.

MacAyeal D. R., Abbot D. S., Siergienko O. V., 2011, *Iceberg-capsize tsunami genesis*, Ann. Glaciol., 52 (58), 51–56, http://dx.doi.org/10.3189/172756411797252103.

Massel S. R., 1967, *Distribution of pressure-impulse on a cylindrical vessel body during side launching*, Rozpr. Hydr., 20, 37–52, (in Polish).

Massel S. R., 2012, *Tsunami in coastal zone due to meteorite impact*, Coast. Eng., 66, 40–49, http://dx.doi.org/10.1016/j.coastaleng.2012.03.013.

Nelson R. C., 1996, *Hydraulic roughness of coral reef platforms*, Appl. Ocean Res., 18, 265–274, http://dx.doi.org/10.1016/S0141-1187(97)00006-0.

Newman J. N., 1977, *Marine hydrodynamics*, The MIT Press, Cambridge, 367 pp.

Noda E., 1970, *Water waves generated by landslides*, J. Waterw. Port C. Div., 96 (4), 835–855.

Oerlemans J., Jania J., Kolendra L., 2011, *Application of a minimal glacier model to Hansbreen, Svalbard*, The Cryosphere, 5, 1–11, http://dx.doi.org/10.5194/tc-5-1-2011.

Peng W., Peregrine D. H., 2000, *Pressure-impulse theory for plate impact on water surface*, Proc. 15 Int. Workshop on Water Waves and Floating Bodies, Caesarea, 146–149.

Piessens R., 1996, *The Hankel transform*, [in:] *The transforms and applications handbook*, A. D. Poularikas (ed.), 2nd edn., CRC Press, Boca Raton, 1336 pp.

Schlichting H., 1960, *Boundary layer theory*, McGraw Hill Book Co., New York, 647 pp.

Stanley S. J., Jenkins A., Guilivi C. F., Dutrieux P., 2011, *Stronger ocean circulation and increased melting under Pine Island Glacier ice shelf*, Nat. Geosci., 4 (8), 519–523, http://dx.doi.org/10.1038/ngeo1188.

Stoker J., 1957, *Water waves*, Intersci. Publ., New York, 567 pp.